Hine, A.C., Feary, D.A., and Malone, M.J. (Eds.)
Proceedings of the Ocean Drilling Program, Scientific Results Volume 182

14. Data Report: Mineralogy and Geochemistry of ODP Site 1128, Great Australian Bight[1]

David J. Mallinson,[2] Benjamin A. Flower,[3] Albert C. Hine,[3] Gregg R. Brooks,[4] Roberto Molina Garza,[5] Tina M. Drexler,[4] and the Leg 182 Shipboard Scientific Party[6]

ABSTRACT

This report presents mineralogic and geochemical data from Ocean Drilling Program Leg 182 Site 1128 in the Great Australian Bight. Clay mineralogy is dominated by mixed-layer illite-smectite, followed by minor amounts of kaolinite and illite, with intervals of pure smectite. Carbonate mineralogy is exclusively low-Mg calcite, except for one interval of dolomite in lower Oligocene sediments. Carbonate increases significantly in upper Eocene sediments, decreases through the lower Oligocene, then increases again in the Neogene. Quartz is present as a minor component that covaries inversely with carbonate. High-resolution sampling associated with Chron 13 normal (early Oligocene) reveals high-frequency (~23 k.y.) fluctuations in clay mineralogy and carbonate abundance and a positive oxygen and carbon isotope excursion (in bulk carbonates) related to Antarctic glaciation.

INTRODUCTION

The objective of this report is to establish a low-resolution record of the evolution of the Australian-Antarctic seaway (AAS) from a juvenile to a mature basin using mineralogic criteria. Specifically, we have determined the mineralogy of the carbonate and noncarbonate fractions of the Cenozoic section at Leg 182 Site 1128 in the Great Australian Bight (GAB) to understand how the mineralogy of sediments varies through

[1]Mallinson, D.J., Flower, B., Hine, A., Brooks, G.R., Garza, R.M., Drexler, T., and the Leg 182 Shipboard Scientific Party, 2003. Data report: Mineralogy and geochemistry of ODP Site 1128, Great Australian Bight. *In* Hine, A.C., Feary, D.A., and Malone, M.J. (Eds.), *Proc. ODP, Sci. Results,* 182, 1–17 [Online]. Available from World Wide Web: <http://www-odp.tamu.edu/publications/182_SR/VOLUME/CHAPTERS/001.PDF>. [Cited YYYY-MM-DD]
[2]Department of Geology, East Carolina University, Greenville NC 27858, USA. Correspondence author: **mallinsond@mail.ecu.edu**
[3]College of Marine Science, University of South Florida, St. Petersburg FL 33701, USA.
[4]Department of Marine Science, Eckerd College, St. Petersburg FL 33711, USA.
[5]Unidad de Ciencias de la Tierra, Campus Juriquilla UNAM, Juriquilla, Queretaro, Mexico 76230.
[6]Shipboard Scientific Party addresses.

Initial receipt: 10 April 2001
Acceptance: 23 September 2002
Web publication: 3 February 2003
Ms 182SR-001

time. We have also produced a high-resolution (~1 sample/5 k.y.) record of clay mineralogy and isotope geochemistry from early Oligocene sediments corresponding to Chron 13 normal.

SETTING

Site 1128 is the deepwater site for Leg 182 in the GAB. This site is located on the upper continental rise in 3874.4 m of water (Fig. F1). An overview of the sedimentary section is presented in the Leg 182 *Initial Reports* volume (Feary, Hine, Malone, et al., 2000).

F1. Map of the GAB, p. 6.

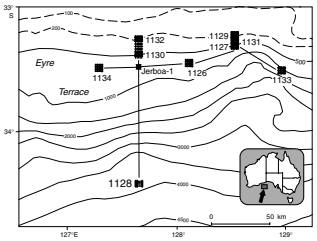

METHODS

Samples were separated into >63-, 263-, and <2-µm size fractions by sieving and centrifuging. Mineralogic analyses were performed at the College of Marine Science, University of South Florida, using a Scintag XDS 2000 X-ray diffractometer on oriented and glycolated clays and grain-size separates. For clay analyses, samples were scanned from 2° to 40° 2θ. For carbonate analyses, samples were scanned from 25° to 32° 2θ. Clay abundance was determined on a relative semiquantitative basis by determining the area (counts per second integrated over degrees 2θ) under the 001 peak on X-ray diffraction records. Peak areas were summed for all clay minerals present within a sample, then each peak area was divided by the sum to arrive at a peak-area ratio. The peak-area ratio should not be confused with percent abundance but does provide a useful tool for determining relative mineralogic variations downcore. Likewise, the quartz peak area (3.34-Å peak) was determined in each sample to provide the relative variation in quartz abundance downcore. Total carbonate was measured on bulk samples using acid digestion and filtration methods.

Carbon and oxygen isotopic investigations of bulk carbonate samples were performed at the College of Marine Science, University of South Florida, using a Finnigan/MAT DeltaPlus XL isotope ratio mass spectrometer equipped with a Kiel III automated carbonate preparation device. Bulk sediment samples were first baked in vacuum at 350°C for 1 hr to deactivate organic carbon prior to acid digestion. All measurements are reported as per mil relative to the Peedee belemnite (PDB) carbonate standard. External precision (based on over 400 NBS-19 standard runs since July 2000) is ±0.04 for $\delta^{13}C$ and ±0.06 for $\delta^{18}O$.

T1. Mineralogy and grain-size data, p. 10.

RESULTS

All biostratigraphic and lithostratigraphic data are from the Leg 182 *Initial Reports* volume (Feary, Hine, Malone, et al., 2000). All mineralogy and grain-size data are presented in Table T1. The carbonate fraction at this deepwater site is exclusively low-Mg calcite (LMC) derived from nannofossils. The primary focus of this report is the variation in the mineralogy of the clay fraction and variations in carbonate and quartz abundance. Figure F2 reveals long-term trends and relationships among data. Natural gamma data collected during downhole logging are also presented for comparative purposes.

Initial visual core descriptions from Site 1128 reveal a succession of sedimentary facies from Paleogene siliciclastics (green sandy siltstones

F2. Clay mineralogy, quartz abundance, natural gamma, and carbonate data, p. 7.

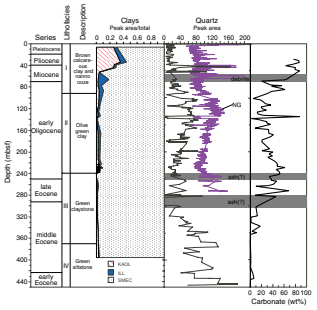

to green claystones) to Neogene calcareous sediments. These sedimentary facies reflect processes occurring in the source regions (relief, rates and styles of weathering, climate, etc.) as well as processes occurring within the depositional environment (energy, diagenesis, water column chemistry, productivity, etc.). The various parameters that controlled sedimentary facies in the GAB clearly evolved throughout the Cenozoic in response to the progressive northward drift of Australia to lower latitudes, the influence of the ever-widening AAS, and global paleoclimatic and paleoceanographic transitions, such as the establishment of surface and deepwater flow through the AAS, and expansion of the East Antarctic Ice Sheet (Shackleton and Kennett, 1975; Miller et al., 1991; Zachos et al., 1996; Robert and Kennett, 1997).

Clay Mineralogy

Clay minerals throughout the sedimentary column at Site 1128 are dominated by smectite, with varying amounts of illite interlayers (0%–30%). On average, kaolinite is the second most abundant clay mineral (in terms of peak-area ratio) followed by discrete illite. However, peak-area ratios of illite do exceed kaolinite in certain intervals (Fig. F2).

Smectite and kaolinite are the dominant clay minerals in the early–middle Eocene section (Fig. F2; Table T1). A possible bentonite layer consisting of smectite with minor kaolinite marks the middle/upper Eocene boundary (Fig. F2). The upper Eocene section is characterized by a small increase in illite concentrations.

The clay mineralogic record between 260 and 240 meters below seafloor (mbsf) (across the Eocene/Oligocene boundary) consists of pure smectite (0% mixed layers), except for a very minor fraction of kaolinite at 250 mbsf. At 240 mbsf, there is a sudden reappearance and rapid increase of kaolinite and illite and mixed-layer illite-smectite (Fig. F3). Between 240 and 210 mbsf, kaolinite and illite covary, with periods of ~23 k.y. (Fig. F4), based on our age model (see "Early Oligocene Age Model," p. 4). The clay mineral oscillations are roughly antiphase, with the carbonate percentage and color reflectance oscillations (Fig. F3).

There is a general increase in illite and kaolinite from 140 to 68 mbsf (late–early Oligocene). Then, between 53 and 43 mbsf (late Miocene), there is a significant increase in kaolinite.

Quartz Abundance

The peak area of the 001 quartz reflector was determined on all samples to provide some indication of quartz variability. These data are presented in Table T1 and Figure F2. Variations in the quartz peak area closely correspond to the natural gamma (NG) log, indicating that the NG log is responding primarily to the abundance of terrigenous minerals. Quartz is most abundant in Lithofacies IV (the green siltstone facies), corresponding to early–middle Eocene time. There is a general decrease in the quartz peak area during this time interval, with no quartz found at the middle/upper Eocene boundary. Above this boundary, quartz increases into the mid–early Oligocene then decreases upward through the Neogene section, with two brief peaks in the Miocene and at the Miocene/Pliocene boundary.

F3. Isotopic and mineralogic data, p. 8.

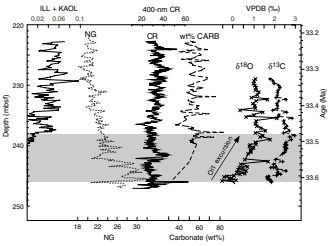

F4. Results of spectral analyses of terrigenous clays and carbonate, p. 9.

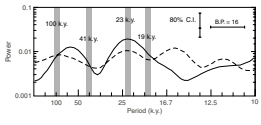

Carbonate Abundance

Carbonate generally varies inversely to the quartz abundance and NG intensity (Fig. F2). Except for a 4-m-thick interval of nonstoichiometric dolomite in lower Oligocene sediments, all carbonate found at Site 1128 consisted of the LMC polymorph. Carbonate shows a minimum (<20% wt%) from 450 to ~290 mbsf (early–middle Eocene). There is a marked increase in carbonate across the middle Eocene/upper Eocene boundary. The upper Eocene is marked by very high amplitude fluctuations (10% to >40%) in carbonate percentage. The early Oligocene record at Site 1128 reveals initially high carbonate percentages corresponding to a 20-m-thick nannofossil chalk unit (Hine et al., 1999; Feary, Hine, Malone, et al., 2000). Above the Eocene/Oligocene boundary (~250 mbsf), carbonate abundance stabilizes somewhat at values of between 40% and 50%. Carbonate then decreases from ~230 to 130 mbsf (most of the lower Oligocene), and increases during the Neogene.

Early Oligocene Age Model

Our age model (Fig. F3; Table T2) is based upon the geomagnetic polarity timescale of Berggren et al. (1995) and is constrained by the presence of the base of Chron 13n (33.545 Ma) at 241.8 ± 1 mbsf at Holes 1128B and 1128D and the top of Chron C13n (33.058 Ma) at 213.5 ± 0.2 mbsf (Feary, Hine, Malone, et al., 2000). Sample ages were linearly interpolated between these two horizons. The resulting accumulation rate is 58 m/m.y. Biostratigraphic data confirm an early Oligocene age but are poorly constrained in this section.

T2. Age and isotopic data from the Oi1 interval, p. 17.

Early Oligocene Oxygen and Carbon Isotopes

Bulk carbonate isotopic data from early Oligocene sediments (228–246 mbsf) reveal a well-defined +2‰ $\delta^{18}O$ shift, with the steepest gradient between 33.6 and 33.48 Ma (Fig. F3; Table T2), consistent with the findings of Zachos et al. (1996). The $\delta^{13}C$ shift is less well defined but occurs in several steps that coincide with the $\delta^{18}O$ shift (Fig. F3). The $\delta^{18}O$ excursion corresponds precisely with the decrease in NG and the increase in carbonate percentages.

ACKNOWLEDGMENTS

The authors would like to thank Co-Chief Scientist David Feary and Staff Scientist Mitchell Malone of Leg 182. We also thank the staff of the Ocean Drilling Program (ODP) Core Repository at Texas A&M University for their assistance and hospitality during subsampling. This research used samples and/or data provided by the ODP. ODP is sponsored by the U.S. National Science Foundation (NSF) and participating countries under management of Joint Oceanographic Institutions (JOI), Inc. Funding for this research was provided by JOI/United States Science Support Program Grant 182-F001025.

REFERENCES

Berggren, W.A., Kent, D.V., Swisher, C.C., III, and Aubry, M.-P., 1995. A revised Cenozoic geochronology and chronostratigraphy. *In* Berggren, W.A., Kent, D.V., Aubry, M.-P., and Hardenbol, J. (Eds.), *Geochronology, Time Scales and Global Stratigraphic Correlation*. Spec. Publ.—SEPM, 54:129–212.

Feary, D.A., Hine, A.C., Malone, M.J., et al., 2000. *Proc. ODP, Init. Repts.,* 182 [CD-ROM]. Available from: Ocean Drilling Program, Texas A&M University, College Station, TX 77845-9547, U.S.A.

Hine, A.C., Feary, D.A., Malone, M.J., Andres, M., Betzler, C., Brooks, G.R., Brunner, C.A., Fuller, M.D., Holbourn, A.E., Huuse, M., Isern, A.R., James, N.P., Ladner, B.C., Li, Q., Machiyama, H., Mallinson, D.J., Matsuda, H., Mitterer, R.M., Molina, G.R.S., Robin, C., Russell, J.L., Shafik, S., Simo, J.A.T., Smart, P.L., Spence, G.H., Surlyk, F., Swart, P.K., and Wortmann, U.G., 1999. Research in the Great Australian Bight yields exciting early results. *Eos,* 80:521.

Miller, K.G., Wright, J.D., and Fairbanks, R.G., 1991. Unlocking the Ice House: Oligocene-Miocene oxygen isotopes, eustasy, and margin erosion. *J. Geophys. Res.,* 96:6829–6848.

Robert, C., and Kennett, J.P., 1997. Antarctic continental weathering changes during Eocene-Oligocene cryosphere expansion: clay mineral and oxygen isotope evidence. *Geology,* 25:587–590.

Shackleton, N.J., and Kennett, J.P., 1975. Paleotemperature history of the Cenozoic and the initiation of Antarctic glaciation: oxygen and carbon isotope analyses in DSDP Sites 277, 279, and 281. *In* Kennett, J.P., Houtz, R.E., et al., *Init. Repts. DSDP,* 29: Washington (U.S. Govt. Printing Office), 743–755.

Zachos, J.C., Quinn, R.M., and Salamy, K., 1996. High resolution (10^4 yr) deep-sea foraminiferal stable isotope records of the Eocene-Oligocene climate transition. *Paleoceanography,* 11:251–266.

Figure F1. Map of the GAB area showing the bathymetry and location of sites drilled during Leg 182.

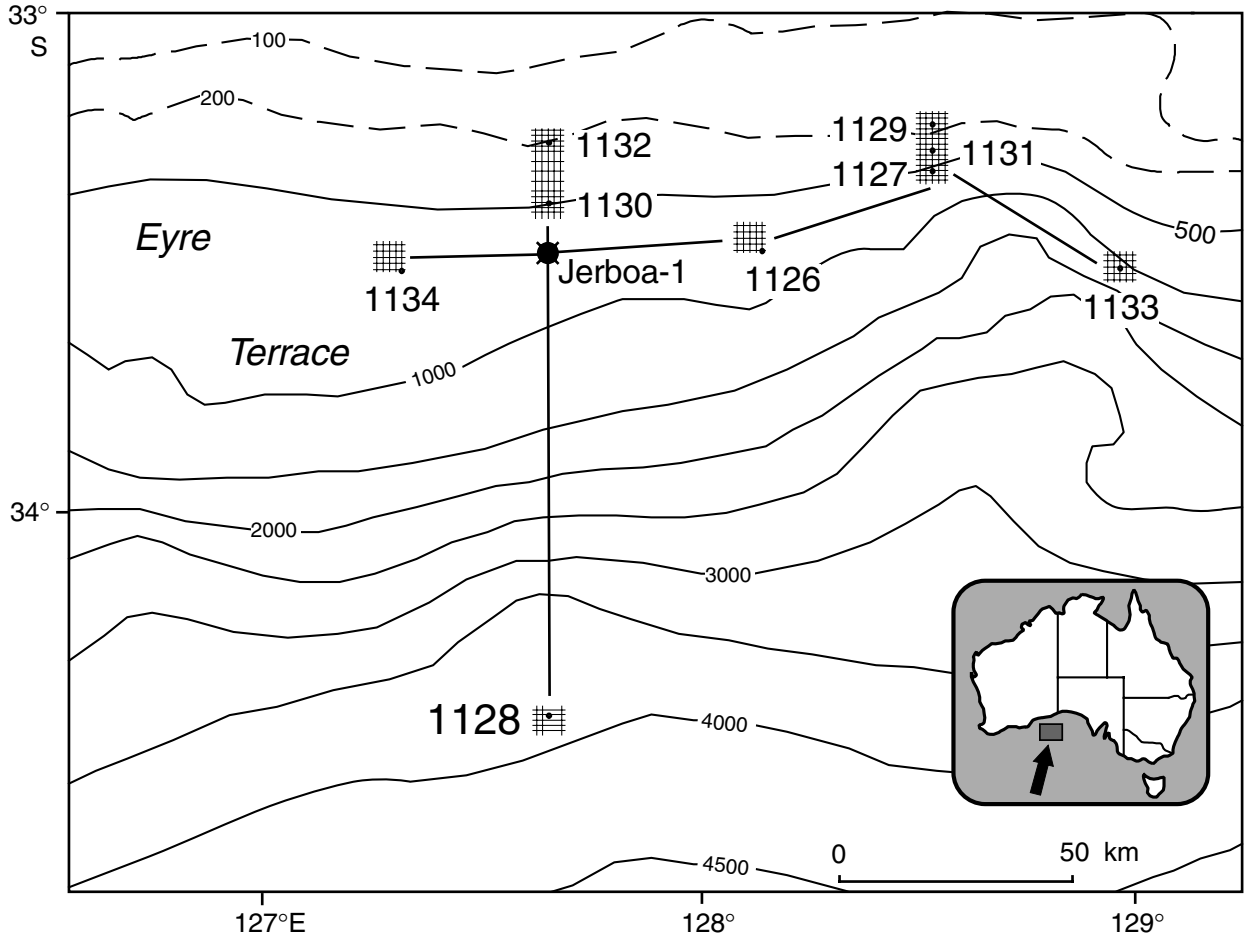

Figure F2. Clay mineralogy, quartz abundance, natural gamma, and weight percent carbonate data from Holes 1128B and 1128D. Peak areas for quartz and clays are counts per second integrated over degrees 2θ. Lithofacies and ages are also presented.

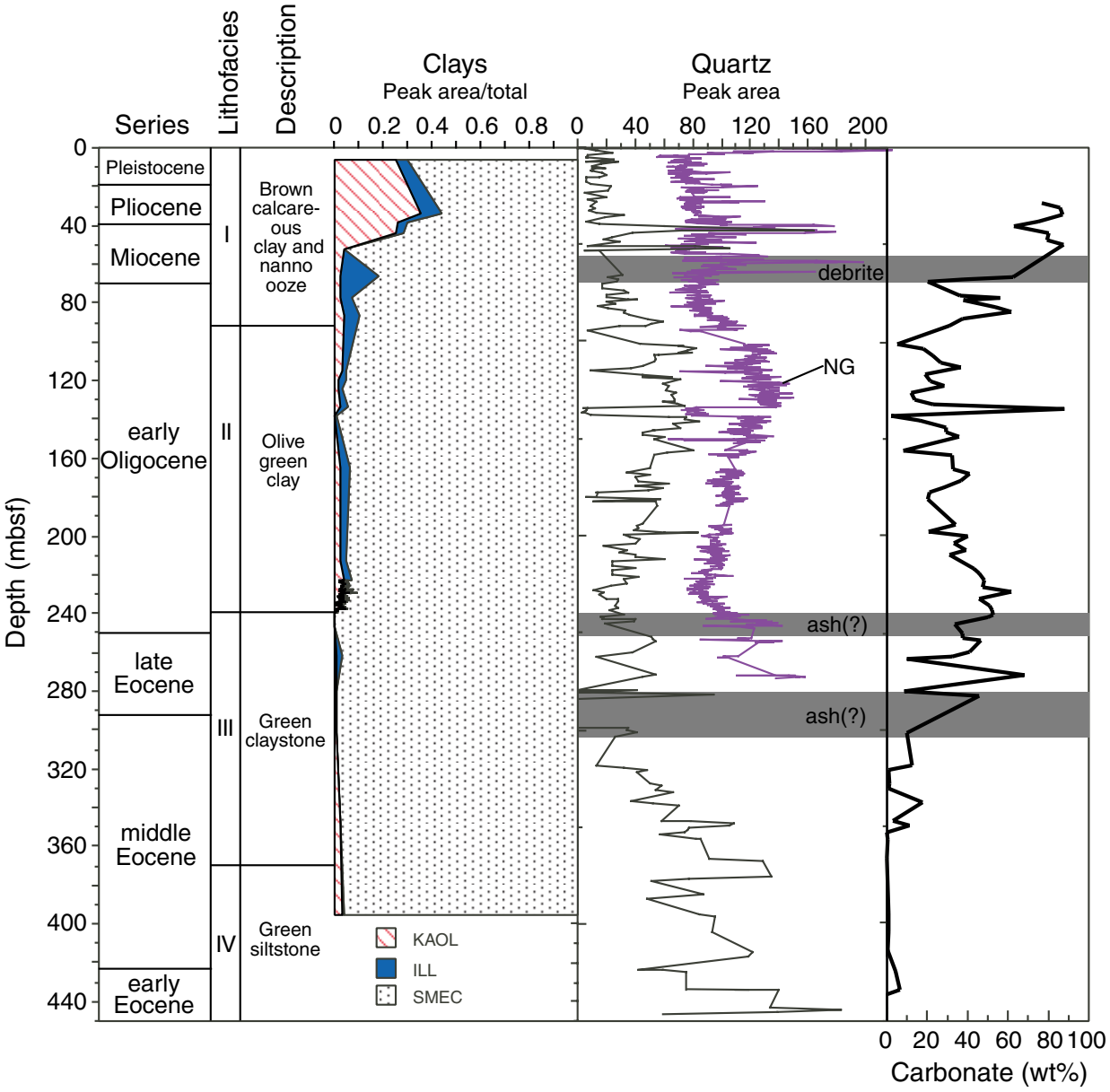

Figure F3. Isotopic and mineralogic data from the lower Oligocene sediments at Hole 1128B. Data shown include clay ratios (illite [ILL] + kaolinite [KAOL]), natural gamma (NG), 400-nm color reflectance (CR), weight percent carbonate, and carbon and oxygen isotopes from bulk carbonate samples. Depth units are in mbsf. The age scale is constrained by the upper and lower boundaries of Chron C13n (see **"Early Oligocene Age Model,"** p. 4). VPDB = Vienna Peedee belemnite.

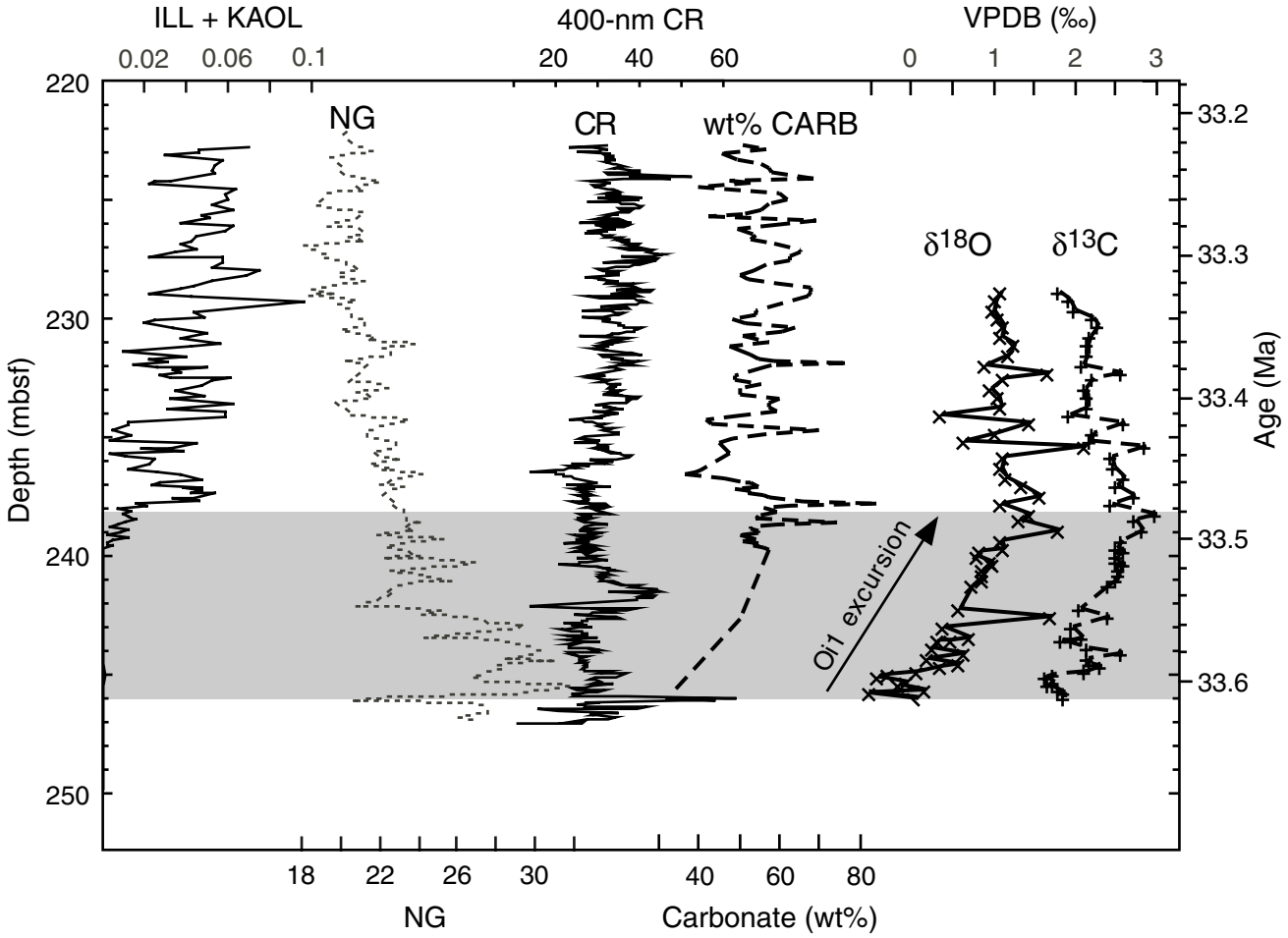

Figure F4. Results of spectral analyses of the terrigenous clays (illite + kaolinite; solid line) and weight percent carbonate (dashed line) from 33.2 to 33.5 Ma. Expected Milankovitch periods are delineated by the vertical gray bars. The 80% confidence interval (C.I.) and bandpass width (B.P.) are also shown.

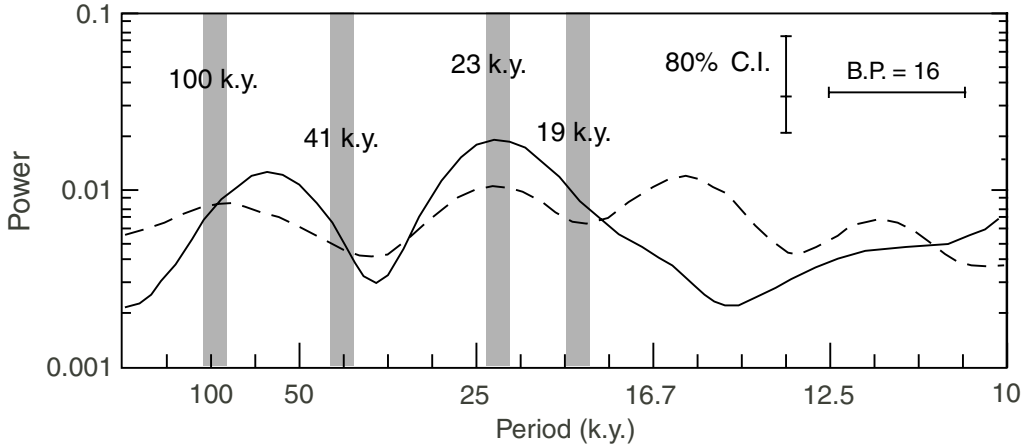

Table T1. Mineralogy and grain-size data, Holes 1128B and 1128D. (**See table note.** Continued on next six pages.)

Core, section, interval (cm)	Depth (mbsf)	$CaCO_3$ (wt%)	Quartz peak area	Smectite* (%)	Illite* (%)	Kaolinite* (%)	Sand (wt%)	Silt (wt%)	Clay (wt%)	Mean (ϕ)
182-1128B-										
1H-1, 20–22	0.20		64.60							
1H-1, 25–27	0.25		5.20							
1H-1, 110–112	1.10		13.50							
1H-2, 20–22	1.70		14.30							
1H-2, 110–112	2.60		24.10							
1H-3, 20–22	3.20		7.40							
1H-3, 110–112	4.10		6.40							
1H-4, 20–22	4.70		7.40							
1H-4, 25–27	4.75		6.20							
2H-1, 32–34	6.02		25.10							
2H-1, 41–43	6.11			0.70	0.04	0.25				
2H-1, 110–112	6.80		6.30							
2H-2, 19–21	7.39		28.50							
2H-2, 110–112	8.30		15.70							
2H-3, 19–21	8.89		10.50							
2H-3, 110–112	9.80		19.00							
2H-4, 19–21	10.39		9.60							
2H-4, 25–27	10.45		12.00							
2H-4, 110–112	11.30		10.10							
2H-5, 19–21	11.89		8.70							
2H-5, 110–112	12.80		16.70							
2H-6, 110–112	14.30		20.30							
2H-7, 15–17	14.85		15.00							
3H-1, 18–20	15.38		6.50							
3H-2, 18–20	16.88		6.50							
3H-3, 18–20	18.38		9.30							
3H-4, 18–20	19.88		22.80							
3H-5, 18–20	21.38		21.40							
3H-6, 18–20	22.38		4.80							
4H-1, 19–21	24.89		20.30							
4H-1, 60–61	25.30	88.2								
4H-2, 19–21	26.39		7.20							
4H-3, 19–21	27.89		13.10							
4H-3, 60–61	28.30	76.7								
4H-4, 19–21	29.39		8.60							
4H-5, 19–21	30.89		11.60							
4H-5, 60–61	31.30	85.6								
4H-6, 19–21	32.39		8.40							
4H-7, 19–21	33.09		13.40							
5H-1, 19–21	34.39		32.10							
5H-1, 25–27	34.45			0.56	0.09	0.36				
5H-1, 57–58	34.77	87.0								
5H-2, 19–21	35.89		18.90							
5H-3, 19–21	37.39		6.50							
5H-3, 59–60	37.79	75.1								
5H-4, 19–21	38.89		15.50							
5H-4, 25–27	38.95			0.70	0.04	0.26				
5H-5, 19–21	40.39		60.50							
5H-5, 58–59	40.78	63.0								
5H-6, 19–21	41.89		163.80							
5H-7, 19–21	42.89		71.90							
6H-1, 60–61	44.30	80.2								
6H-1, 18–20	43.88		38.60							
6H-1, 37–39	44.07			0.72	0.03	0.25				
6H-2, 18–20	45.38		23.70							
6H-3, 18–20	46.88		17.90							
6H-3, 60–61	47.30	79.3								
6H-4, 18–20	48.38		29.00							
6H-5, 18–20	49.88		6.70							
6H-5, 60–61	50.30	87.7								
6H-5, 110–112	50.80		81.70							
6H-6, 18–20	51.38		106.00							
6H-6, 110–112	52.30		4.90							
6H-7, 18–20	52.88		14.60	0.96	0.00	0.04				
8H-2, 110–112	65.30		30.90							
8H-3, 18–20	65.88		21.20							

Table T1 (continued).

Core, section, interval (cm)	Depth (mbsf)	$CaCO_3$ (wt%)	Quartz peak area	Smectite* (%)	Illite* (%)	Kaolinite* (%)	Sand (wt%)	Silt (wt%)	Clay (wt%)	Mean (ϕ)
8H-3, 59–60	66.29	62.4								
8H-3, 110–111	66.8			0.82	0.15	0.03				
8H-4, 18–20	67.38		28.20							
8H-4, 58–59	67.78	37.8								
8H-5, 18–20	68.88		27.30							
8H-5, 59–60	69.29	20.4								
8H-6, 18–20	70.38		17.20							
8H-7, 18–20	71.88		17.30							
9H-1, 110–112	73.30		32.50							
9H-2, 110–112	74.80		34.80							
9H-3, 18–20	75.38		20.10							
9H-3, 59–60	75.79	36.1								
9H-4, 18–20	76.88		20.30							
9H-4, 34–35	77.04	55.9		0.93	0.05	0.02				
9H-4, 110–112	77.80		34.70							
9H-5, 18–20	78.38		41.10							
9H-5, 59–60	78.79	37.9								
9H-5, 110–112	79.30		19.80							
9H-6, 18–20	79.88		26.20							
9H-7, 18–20	81.38		13.80							
10H-1, 18–20	81.88		20.90							
10H-1, 59–60	82.29	53.9								
10H-2, 18–20	83.38		33.30							
10H-3, 18–20	84.88		31.70							
10H-3, 59–60	85.29	61.5								
10H-4, 18–20	86.38		36.30							
10H-4, 25–27	86.45			0.90	0.06	0.04				
10H-5, 18–20	87.88		49.20							
10H-5, 59–60	88.29	37.3								
10H-6, 18–20	89.38		58.80							
10H-7, 18–20	90.88		50.90							
11H-1, 20–22	91.40		47.20							
11H-1, 25–27	91.45		29.20							
11H-1, 60–61	91.80	30.9								
11H-2, 110–112	93.80		6.90							
12H-1, 18–20	100.88		43.40							
12H-1, 60–61	101.30	5.0								
12H-1, 110–112	101.80		73.60							
12H-2, 18–20	102.38		69.90							
12H-2, 110–112	103.30		82.30							
12H-3, 18–20	103.88		76.10							
12H-3, 60–61	104.30	18.3								
12H-3, 110–112	104.80		70.40							
12H-4, 18–20	105.38		78.90							
12H-4, 110–112	106.30		56.30							
12H-5, 18–20	106.88		53.10							
12H-5, 60–61	107.30	22.8								
12H-6, 110–112	109.30		54.50							
13H-1, 18–20	110.38		53.60							
13H-1, 60–61	110.80	26.6								
13H-2, 18–20	111.88		45.50							
13H-3, 18–20	113.38		37.40							
13H-3, 60–61	113.80	36.7								
13H-4, 18–20	114.88		9.50							
13H-4, 25–27	114.95			0.95	0.02	0.03				
13H-5, 18–20	116.38		44.90							
13H-5, 60–61	116.80	18.8								
13H-6, 18–20	117.88		65.20							
13H-7, 18–20	119.38		71.40							
14H-1, 18–20	117.88		45.10							
14H-1. 25–27	119.95			0.95	0.03	0.01				
14H-1, 60–61	120.30	21.6								
14H-2, 18–20	121.38		59.00							
14H-3, 18–20	122.88		62.90							
14H-3, 60–61	123.30	28.5								
14H-4, 18–20	124.38		61.40							
14H-4, 25–27	124.45			0.96	0.02	0.01				
14H-5, 18–20	125.88		68.50							

Table T1 (continued).

Core, section, interval (cm)	Depth (mbsf)	$CaCO_3$ (wt%)	Quartz peak area	Smectite* (%)	Illite* (%)	Kaolinite* (%)	Sand (wt%)	Silt (wt%)	Clay (wt%)	Mean (ϕ)
14H-5, 60–61	126.30	12.1								
14H-6, 18–20	127.38		65.10							
14H-7, 18–20	128.88		67.30							
15H-1, 110–112	130.30		67.20							
15H-1, 60–61	129.80	13.6								
15H-2, 18–20	130.88		58.80							
15H-2, 110–112	131.80		69.30							
15H-3, 18–20	132.38		74.40							
15H-3, 60–61	132.80	23.0								
15H-4, 18–20	133.47		3.60							
15H-4, 25–27	133.54			0.94	0.03	0.03				
15H-4, 110–112	134.39		7.40							
15H-5, 18–20	134.94		6.40							
15H-5, 60–61	135.36	88.0								
15H-5, 110–112	135.86		2.60							
15H-6, 18–20	136.44		4.80							
15H-6, 110–112	137.36		8.60							
16X-1, 18–20	137.98		63.60							
16X-1, 25–27	138.05			0.99	0.01	0.00				
16X-1, 60–61	138.40	2.1								
16X-1, 110–112	138.90		75.00							
16X-2, 18–20	139.48		74.50							
16X-3, 18–20	140.98		84.70							
16X-3, 60–61	141.40	16.5								
16X-4, 18–20	142.48		66.80							
16X-5, 18–20	143.98		71.40							
16X-5, 60–61	144.40	29.1								
16X-6, 18–20	145.48		52.00							
16X-7, 18–20	146.98		44.90							
17X-1, 18–20	145.98		53.40							
17X-1, 60–61	146.40	29.5								
17X-2, 18–20	147.48		45.30							
17X-3, 19–21	148.99		60.10							
17X-3, 59–60	149.39	35.9								
17X-4, 18–20	150.48		53.40							
18X-1, 18–20	155.58		80.20							
18X-1, 60–61	156.00	8.4								
18X-2, 18–20	157.08		62.80							
18X-3, 18–20	158.58		53.30							
18X-3, 60–61	159.00	32.3								
19X-1, 18–20	165.28		50.10							
19X-1, 25–27	165.35			0.94	0.04	0.02				
19X-1, 60–61	165.70	32.6								
19X-2, 18–20	166.78		34.50							
19X-3, 18–20	168.28		50.00							
19X-3, 60–61	168.70	40.9								
19X-4, 18–20	169.78		40.30							
19X-5, 18–20	171.28		41.80							
19X-5, 60–61	171.70	36.8								
19X-6, 18–20	172.78		63.50							
19X-7, 18–20	174.28		40.70							
20X-1, 18–20	174.88		58.90							
20X-1, 60–61	175.30	27.9								
20X-2, 18–20	176.38		49.50							
20X-2, 110–112	177.30		12.90							
20X-3, 18–20	177.88		13.80							
20X-3, 60–61	178.30	21.1								
20X-4, 18–20	179.38		13.40							
20X-4, 110–112	180.30		5.70							
20X-5, 18–20	180.88		57.70							
20X-5, 60–61	181.30	20.4								
20X-5, 110–112	181.80		11.40							
20X-6, 18–20	182.38		54.50							
20X-7, 18–20	183.88		55.20							
22X-1, 18–20	194.08		45.30							
22X-1, 60–61	194.50	34.0								
22X-1, 110–112	195.00		40.80							
22X-2, 18–20	195.58		41.90							

Table T1 (continued).

Core, section, interval (cm)	Depth (mbsf)	$CaCO_3$ (wt%)	Quartz peak area	Smectite* (%)	Illite* (%)	Kaolinite* (%)	Sand (wt%)	Silt (wt%)	Clay (wt%)	Mean (ϕ)
22X-3, 18–20	197.08		39.50							
22X-3, 60–61	197.50	20.8								
22X-3, 110–112	198.00		59.80							
22X-4, 18–20	198.58		83.90							
22X-4, 110–112	199.50		32.30							
22X-5, 18–20	200.08		36.40							
22X-5, 60–61	200.50	40.1								
22X-6, 18–20	201.58		42.80							
23X-1, 19–21	203.69		40.20							
23X-1, 60–62	204.10	33.1								
23X-2, 19–21	205.19		17.90							
23X-3, 19–21	206.69		34.50							
23X-3, 60–62	207.10	39.2								
23X-4, 19–21	208.19		29.50							
23X-5, 19–21	209.69		39.80							
23X-5, 60–62	210.10	31.0								
23X-6, 19–21	211.19		40.70							
23X-7, 19–21	212.39		60.00							
24X-1, 18–20	213.28		24.30							
24X-1, 26–28	213.36			0.95	0.02	0.02				
24X-1, 60–61	213.70	37.2								
24X-2, 18–20	214.78		24.50							
24X-3, 18–20	216.28		39.80							
24X-3, 64–65	216.74	43.2								
24X-4, 18–20	217.78		23.90							
24X-5, 18–20	219.28		23.70							
24X-5, 64–65	219.74	45.9								
24X-6, 18–20	220.78		41.90							
24X-7, 18–20	222.28		32.10							
25X-1, 2–4	222.72	50.6		0.93	0.03	0.04				
25X-1, 20–22	222.9	56.8		0.95	0.01	0.04				
25X-1, 25–27	222.95			0.95	0.02	0.02				
25X-1, 40–42	223.1	45.9		0.97	0.01	0.02				
25X-1, 59–60	223.29	48.2								
25X-1, 60–62	223.3	49.5		0.94	0.02	0.04				
25X-1, 80–82	223.5	55.2		0.95	0.03	0.03				
25X-1, 102–104	223.72	57.1		0.95	0.02	0.03				
25X-1, 120–122	223.9	58.1		0.95	0.02	0.04				
25X-1, 148–150	224.18	68.5		0.97	0.01	0.03				
25X-2, 2–4	224.22	47.9		0.97	0.01	0.02				
25X-2, 10–12	224.3	53.0		0.98	0.01	0.01				
25X-2, 18–20	224.38		34.10							
25X-2, 30–32	224.5	40.0		0.94	0.03	0.04				
25X-2, 40–42	224.6	46.6		0.94	0.03	0.03				
25X-2, 60–62	224.8	60.3		0.94	0.02	0.04				
25X-2, 80–82	225	62.2		0.94	0.02	0.04				
25X-2, 102–104	225.22	57.4		0.95	0.02	0.03				
25X-2, 122–124	225.42	55.2		0.94	0.02	0.04				
25X-2, 140–142	225.6	51.1		0.95	0.02	0.03				
25X-3, 2–4	225.72	42.6		0.95	0.03	0.03	0.9	74.8	24.3	6.4
25X-3, 18–20	225.88		22.80							
25X-3, 22–24	225.92	69.4		0.96	0.01	0.02	0.3	66.9	32.7	6.9
25X-3, 40–42	226.1	59.2		0.94	0.03	0.04	0.3	60.7	39.1	7.3
25X-3, 59–60	226.29	47.3								
25X-3, 60–62	226.3	49.4		0.94	0.03	0.03	0.6	63.8	35.5	7.1
25X-3, 80–82	226.5	54.3		0.96	0.02	0.03	0.3	61.1	38.6	7.3
25X-3, 100–102	226.7	52.8		0.96	0.01	0.03	0.5	98.4	1.1	5.1
25X-3, 120–122	226.9	58.9		0.96	0.01	0.03	0.3	64.0	35.7	7.1
25X-3, 140–142	227.1	65.3		0.96	0.02	0.03	0.2	59.2	40.6	7.4
25X-4, 2–4	227.22	65.5		0.96	0.01	0.03	0.1	55.8	44.1	7.6
25X-4, 18–20	227.38		11.40							
25X-4, 22–24	227.42	62.6		0.98	0.01	0.01	0.2	44.4	55.3	8.3
25X-4, 25–27	227.45			0.94	0.02	0.04				
25X-4, 42–44	227.62	62.5		0.94	0.01	0.04	0.6	56.7	42.7	7.5
25X-4, 60–62	227.8	56.5		0.95	0.01	0.04	0.3	57.6	42.2	7.5
25X-4, 80–82	228	53.2		0.92	0.02	0.05	0.2	75.3	24.5	6.5
25X-4, 100–102	228.2	50.3		0.93	0.03	0.04	0.4	58.3	41.3	7.5
25X-4, 122–124	228.42	52.5		0.95	0.01	0.04	1.2	59.8	39.0	7.3

Table T1 (continued).

Core, section, interval (cm)	Depth (mbsf)	$CaCO_3$ (wt%)	Quartz peak area	Smectite* (%)	Illite* (%)	Kaolinite* (%)	Sand (wt%)	Silt (wt%)	Clay (wt%)	Mean (ϕ)
25X-4, 140–142	228.6	59.7		0.96	0.01	0.04	0.3	53.8	45.9	7.7
25X-5, 2–4	228.72	68.0		0.96	0.02	0.02				
25X-5, 18–20	228.88		17.70							
25X-5, 20–22	228.9	67.7		0.98	0.00	0.02				
25X-5, 40–42	229.1	67.3		0.96	0.01	0.03	0.2	82.5	17.3	6.0
25X-5, 59–60	229.29	61.8								
25X-5, 60–62	229.3			0.90	0.03	0.07	0.4	64.4	35.2	7.0
25X-5, 80–82	229.5						0.2	60.8	39.0	7.3
25X-5, 100–102	229.7	54.3		0.96	0.01	0.04	0.7	68.9	30.3	6.8
25X-5, 120–122	229.9	54.2		0.95	0.01	0.04	0.3	70.8	28.9	6.7
25X-5, 140–142	230.1	48.4		0.97	0.01	0.02	0.5	53.8	45.7	7.7
25X-6, 2–4	230.22	51.6		0.98	0.00	0.02	0.3	61.3	38.4	7.3
25X-6, 18–20	230.38		14.70							
25X-6, 22–24	230.42	63.8		0.97	0.01	0.02	0.2	59.4	40.4	7.4
25X-6, 42–44	230.62	60.7		0.95	0.01	0.04	0.2	60.3	39.5	7.4
25X-6, 60–62	230.8	51.2		0.96	0.03	0.01	0.0	60.5	39.5	7.4
25X-6, 80–82	231	57.5		0.94	0.02	0.04	0.6	61.5	37.9	7.3
25X-6, 100–102	231.2	47.5		0.96	0.02	0.02	0.7	64.2	35.1	7.1
25X-6, 122–120	231.42	50.3		0.99	0.01	0.00	0.8	52.1	37.1	7.2
25X-6, 140–142	231.6	53.0		0.96	0.02	0.02	0.8	61.6	37.6	7.2
25X-7, 2–4	231.72	54.5		0.98	0.01	0.02	0.6	53.8	45.6	7.7
25X-7, 10–12	231.8	58.7		0.97	0.01	0.02	0.6	63.2	36.2	7.2
25X-7, 18–20	231.88		20.50							
25X-7, 20–22	231.9	76.5		0.98	0.00	0.01				
25X-7, 30–32	232	58.0		0.97	0.01	0.01				
25X-7, 40–42	232.1	55.9		0.95	0.02	0.03	0.3	49.9	49.8	8.0
25X-CC, 2–4	232.16			0.97	0.01	0.02				
25X-CC, 10–12	232.24			0.96	0.02	0.02	1.0	53.0	46.0	7.7
25X-CC, 20–22	232.34			0.97	0.01	0.02	0.4	53.1	46.5	7.8
25X-CC, 30–32	232.44			0.97	0.01	0.02	0.4	52.2	47.3	7.8
26X-1, 4–6	232.44	49.0		0.94	0.02	0.04	1.3	63.9	34.8	7.1
26X-1, 18–20	232.58		28.00							
26X-1, 20–22	232.6	48.7		0.95	0.02	0.03	1.2	59.6	39.2	7.3
26X-1, 25–27	232.65			0.95	0.03	0.03				
26X-1, 40–42	232.8	55.2		0.95	0.01	0.03	0.5	54.3	45.2	7.7
26X-1, 60–61	233.00	50.1		0.96	0.02	0.02	0.2	51.1	48.7	7.9
26X-1, 82–84	233.22	50.4		0.95	0.02	0.03	0.4	56.7	42.9	7.6
26X-1, 100–102	233.4	60.1		0.97	0.01	0.02	0.3	56.4	43.3	7.6
26X-1, 120–122	233.6	57.2		0.94	0.03	0.04	0.3	63.1	36.6	7.2
26X-1, 140–142	233.8	57.1		0.97	0.01	0.02				
26X-,2 2–4	233.92	59.4		0.94	0.01	0.05	0.2	52.4	47.3	7.8
26X-2, 18–20	234.08		28.40							
26X-2, 20–22	234.1	50.1		0.94	0.01	0.04	0.2	52.0	47.8	7.9
26X-2, 42–44	234.32	41.7		0.99	0.00	0.01				
26X-2, 60–62	234.5	43.3		0.99	0.00	0.01	1.2	52.7	46.1	7.7
26X-2, 83–85	234.73	69.5		0.99	0.00	0.00				
26X-2, 100–102	234.9	56.2		0.99	0.00	0.01	0.2	51.3	48.5	7.9
26X-2, 122–124	235.12	48.6		1.00	0.00	0.00	0.5	61.0	38.5	7.3
26X-2, 140–142	235.3	44.9		0.96	0.01	0.03	1.3	49.7	49.1	7.9
26X-3, 2–4	235.42			0.97	0.01	0.02	0.4	53.5	46.1	7.8
26X-3, 10–12	235.5			0.98	0.01	0.01	1.0	50.3	48.7	7.9
26X-3, 18–20	235.58		26.60	0.96	0.01	0.03				
26X-3, 40–42	235.8			0.99	0.01	0.01	0.9	59.3	38.8	7.2
26X-3, 53–55	235.93			0.97	0.01	0.02	1.7	62.7	35.6	7.1
26X-3, 60–61	236.00	50.9								
26X-3, 70–72	236.1			0.98	0.00	0.02	0.3	54.9	44.7	7.7
26X-3, 100–102	236.4	40.7		0.99	0.00	0.01	0.8	63.7	35.5	7.1
26X-3, 112–114	236.52	39.4		0.97	0.00	0.02	0.7	61.0	38.3	7.3
26X-3, 122–124	236.62	36.4		0.96	0.02	0.02	0.4	60.8	38.9	7.3
26X-3, 138–140	236.78	46.2		0.95	0.02	0.03	0.2	57.8	41.0	7.4
26X-4, 2–4	236.92	51.4		0.97	0.01	0.02	0.6	20.2	79.2	9.7
26X-4, 10–12	237	53.1		0.98	0.00	0.02	0.6	20.2	79.2	9.7
26X-4, 18–20	237.08		27.90							
26X-4, 20–22	237.1	55.1		0.95	0.02	0.03	0.4	97.1	2.5	5.1
26X-4, 25–27	237.15			0.96	0.01	0.03				
26X-4, 30–32	237.2	49.0		0.95	0.01	0.04	2.6	59.6	37.8	7.1
26X-4, 40–42	237.3	52.7		0.96	0.01	0.03	0.1	36.9	61.8	8.6
26X-4, 50–52	237.4	52.1		0.95	0.01	0.05	0.4	58.6	41.0	7.4

Table T1 (continued).

Core, section, interval (cm)	Depth (mbsf)	$CaCO_3$ (wt%)	Quartz peak area	Smectite* (%)	Illite* (%)	Kaolinite* (%)	Sand (wt%)	Silt (wt%)	Clay (wt%)	Mean (ϕ)
26X-4, 63–65	237.53	56.1		0.96	0.01	0.04	0.5	64.4	35.1	7.1
26X-4, 70–72	237.6	57.2		0.97	0.01	0.03	0.3	99.7	0.0	5.0
26X-4, 82–84	237.72	65.9		0.95	0.00	0.04	0.1	89.6	10.3	5.6
26X-4, 92–94	237.82	84.4		0.98	0.00	0.02	1.5	96.6	1.9	5.1
26X-4, 100–102	237.9	62.4		0.98	0.00	0.02	7.3	67.8	25.0	6.3
26X-4, 112–114	238.02	56.2		0.99	0.00	0.00	0.2	55.9	43.9	7.6
26X-4, 120–122	238.1	58.2		0.99	0.00	0.01	0.1	57.4	42.5	7.5
26X-4, 130–132	238.2	59.2		0.99	0.00	0.01	0.2	61.8	38.0	7.3
26X-4, 148–150	238.38	54.1		0.99	0.00	0.01	1.4	62.0	36.6	7.2
26X-5, 2–4	238.42	54.7		0.98	0.00	0.01	0.2	56.5	43.3	7.6
26X-5, 10–12	238.5	54.4		0.98	0.00	0.01	0.2	64.4	35.4	7.1
26X-5, 18–20	238.58		22.60							
26X-5, 22–24	238.62	74.3		0.99	0.00	0.01	0.2	61.6	38.1	7.3
26X-5, 30–32	238.7	59.6		0.99	0.00	0.01	0.3	42.6	57.1	8.4
26X-5, 40–42	238.8	52.9		1.00	0.00	0.00	0.1	56.8	43.1	7.6
26X-5, 50–52	238.9	52.9		0.99	0.00	0.01	0.2	57.2	42.6	7.5
26X-5, 60–61	239.00	52.3								
26X-5, 61–63	239.01	55.1		0.99	0.00	0.01	0.2	58.3	41.5	7.5
26X-5, 70–72	239.1	54.7		1.00	0.00	0.00	0.3	57.1	42.6	7.5
26X-5, 80–82	239.2	50.1		0.99	0.00	0.01	0.3	55.1	44.6	7.7
26X-5, 90–92	239.3	54.1		1.00	0.00	0.00	0.2	49.3	50.6	8.0
26X-5, 100–102	239.4	50.7		1.00	0.00	0.00	0.3	56.0	43.7	7.6
26X-5, 112–114	239.52	54.6		1.00	0.00	0.00	0.2	56.5	43.3	7.6
26X-5, 122–124	239.62	53.2		1.00	0.00	0.00	5.0	62.0	33.0	6.8
26X-5, 130–132	239.7	55.9		1.00	0.00	0.00	0.5	54.6	44.8	7.7
26X-5, 140–142	239.8	57.7		1.00	0.00	0.00	0.3	58.6	41.0	7.5
26X-6, 18–20	240.08		31.80							
26X-7, 18–20	241.58		15.70							
27X-1, 18–20	242.28		16.80							
27X-1, 20–22	242.3			1.00	0.00	0.00				
27X-1, 60–61	242.70	50.1								
27X-1, 110–112	243.20		40.00							
27X-2, 18–20	243.78		38.80							
27X-2, 20–22	243.8			1.00	0.00	0.00				
27X-3, 18–20	245.28		19.30							
27X-3, 20–22	245.3			1.00	0.00	0.00				
27X-3, 60–61	245.70	33.8								
27X-4, 25–27	246.85			1.00	0.00	0.00				
28X-1, 18–20	251.98		50.90							
28X-1, 59–60	252.39	37.4								
28X-1, 110–112	252.90		52.30							
28X-2, 110–112	254.25		54.40							
29X-1, 18–20	261.68		12.80							
29X-1, 25–27	261.75			0.97	0.02	0.01				
29X-1, 59–61	262.09	32.5								
30X-1, 18–20	271.28		53.90							
30X-1, 60–61	271.70	68.0								
30X-1, 110–112	272.20		45.40							
182-1128D-										
2R-1, 60–61	241.40	52.6								
2R-1, 110–112	241.90		18.40							
3R-1, 59–60	250.99	37.6								
3R-3, 59–60	253.99	46.7								
4R-1, 25–27	260.25		38.50							
4R-1, 59–60	260.59	40.8								
4R-3, 59–60	263.59	10.1								
6R-1, 17–19	279.47		0.00							
6R-1, 23–25	279.53		41.00							
6R-1, 59–60	279.89	8.8								
6R-1, 110–112	280.40		0.00	0.99	0.00	0.01				
6R-2, 18–20	280.98		0.00							
6R-2, 110–112	281.90		94.20							
6R-3, 53–54	282.83	45.9								
6R-4, 18–20	283.48		0.00							
8R-1, 15–17	298.65		0.00							
8R-1, 20–22	298.70		35.50							
8R-2, 18–20	300.18		34.20							
8R-3, 18–20	301.68		40.80	1.00	0.00	0.00				

Table T1 (continued).

Core, section, interval (cm)	Depth (mbsf)	$CaCO_3$ (wt%)	Quartz peak area	Smectite* (%)	Illite* (%)	Kaolinite* (%)	Sand (wt%)	Silt (wt%)	Clay (wt%)	Mean (ϕ)
8R-3, 60–61	302.10	9.9								
8R-4, 18–20	303.18		26.20							
10R-1, 19–21	317.79		13.40							
10R-1, 59–60	318.19	12.6								
10R-2, 19–21	319.29		32.30							
10R-3, 19–21	320.79		48.10							
10R-3, 59–60	321.19	0.8								
10R-4, 19–21	321.79		41.00							
11R-1, 19–21	327.39		50.10							
11R-1, 59–60	327.79	1.4								
11R-2, 19–21	328.89		58.70							
11R-3, 19–21	330.39		54.10							
11R-3, 59–60	330.79	0.8								
11R-4, 19–21	331.59		66.20							
12R-1, 18–20	336.98		37.20							
12R-1, 59–60	337.39	17.5								
12R-1, 110–112	337.90		52.60							
12R-2, 18–20	338.48		70.40							
13R-1, 18–20	346.58		58.40							
13R-1, 59–60	346.99	3.1								
13R-1, 110–112	347.50		78.70	0.97	0.00	0.03				
13R-2, 18–20	348.08		108.90							
13R-3, 18–20	349.58		105.40							
13R-3, 59–60	349.99	11.1								
13R-3, 110–112	350.50		77.20							
13R-4, 18–20	351.08		76.40							
13R-5, 18–20	352.58		74.70							
13R-5, 59–60	352.99	0.2								
13R-6, 18–20	354.08		56.90							
13R-7, 18–20	355.58		82.20							
14R-1, 18–20	356.18		85.40							
14R-1, 59–60	356.59	0.5								
15R-1, 18–20	365.88		91.80							
15R-1, 59–60	366.29	0.1								
15R-2, 18–20	367.38		128.50							
16R-1, 18–20	375.58		134.50							
16R-1, 59–60	375.99									
16R-2, 18–20	376.29		77.70							
16R-3, 18–20	377.79		51.70							
17R-1, 18–20	385.18		87.30							
17R-1, 59–60	385.59									
17R-2, 18–20	386.68		47.80							
18R-1, 18–20	394.88		84.00							
18R-1, 60–61	395.30	0.8								
18R-2, 16–18	395.83		95.30	0.96	0.01	0.03				
19R-1, 20–22	404.60		93.40							
19R-1, 60–61	405.00	1.0								
20R-1, 18–20	414.18		60.90							
20R-1, 25–27	414.25		122.10							
20R-1, 60–61	414.60	0.3								
20R-3, 18–20	416.40		119.00							
21R-1, 19–21	423.89		41.90							
21R-1, 25–27	423.95		59.70							
21R-1, 59–60	424.29	4.4								
21R-1, 110–112	424.80		75.40							
22R-1, 18–20	433.48		75.60							
22R-1, 25–27	433.55		109.10							
22R-1, 60–61	433.90	6.4								
22R-1, 110–112	434.40		140.00							
22R-3, 60–61	436.90	0.1								
23R-1, 14–16	443.04		133.90							
23R-1, 58–59	443.48	0.2								
23R-2, 14–16	444.54		182.90							
23R-2, 110–112	445.50		138.90							
23R-3, 14–16	446.04		59.50							
23R-3, 60–61	446.50	0.1								

Note: * = clay mineral values are a ratio of the clay peak areas (see "Methods," p. 2).

Table T2. Age and isotopic data from the Oi1 interval, Hole 1128B.

Core, section, interval (cm)	Depth (mbsf)	Age* (Ma)	$\delta^{13}C$	$\delta^{18}O$
182-1128B-				
25X-5, 20–22	228.90	33.32	1.78	1.09
25X-5, 60–62	229.30	33.33	1.90	1.01
25X-5, 100–102	229.70	33.34	1.98	0.97
25X-5, 140–142	230.10	33.34	2.19	1.04
25X-6, 22–24	230.42	33.35	2.27	1.12
25X-6, 60–62	230.80	33.36	2.16	1.08
25X-6, 100–102	231.20	33.36	2.13	1.24
25X-6, 140–142	231.60	33.37	2.13	1.17
25X-7, 30–32	232.00	33.38	2.07	0.88
25X-CC, 20–22	232.34	33.38	2.56	1.66
26X-1, 20–22	232.60	33.39	2.19	1.10
26X-1, 60–61	233.00	33.39	2.11	0.96
26X-1, 100–102	233.40	33.40	2.12	1.05
26X-1, 140–142	233.80	33.41	2.14	1.09
26X-2, 20–22	234.10	33.41	1.90	0.34
26X-2, 60–62	234.50	33.42	2.58	1.44
26X-2, 100–102	234.90	33.43	2.20	1.03
26X-2, 140–142	235.30	33.43	2.16	0.64
26X-3, 10–12	235.50	33.44	2.84	2.10
26X-3, 53–55	235.93	33.44	2.43	1.11
26X-3, 100–102	236.40	33.45	2.45	1.07
26X-3, 138–140	236.78	33.46	2.59	1.15
26X-4, 20–22	237.10	33.46	2.48	1.32
26X-4, 63–65	237.53	33.47	2.72	1.57
26X-4, 100–102	237.90	33.48	2.43	1.08
26X-4, 148–150	238.38	33.49	2.97	1.42
26X-5, 22–24	238.62	33.49	2.70	1.29
26X-5, 61–63	239.01	33.50	2.81	1.78
26X-5, 100–102	239.40	33.50	2.55	1.07
26X-5, 140–142	239.80	33.51	2.48	1.11
26X-6, 2–4	239.92	33.51	2.58	0.81
26X-6, 22–24	240.12	33.52	2.50	0.78
26X-6, 42–44	240.32	33.52	2.49	0.94
26X-6, 60–62	240.50	33.52	2.57	0.98
26X-6, 82–84	240.72	33.53	2.52	0.84
26X-6, 100–102	240.90	33.53	2.52	0.86
26X-6, 120–122	241.10	33.53	2.47	0.87
26X-6, 140–142	241.30	33.54	2.39	0.74
27X-1, 20–22	242.30	33.55	2.04	0.58
27X-1, 60–62	242.70	33.56	2.38	1.70
27X-1, 100–102	243.10	33.57	1.95	0.38
27X-1, 140–142	243.50	33.57	2.06	0.69
27X-2, 2–4	243.62	33.58	1.94	0.46
27X-2, 10–12	243.70	33.58	1.83	0.30
27X-2, 40–42	244.00	33.58	2.13	0.25
27X-2, 60–62	244.20	33.59	2.56	0.62
27X-2, 81–83	244.41	33.59	2.13	0.18
27X-2, 100–102	244.60	33.59	2.15	0.55
27X-2, 120–122	244.80	33.60	2.29	0.33
27X-2, 140–142	245.00	33.60	2.10	0.07
27X-3, 2–4	245.12	33.60	1.73	–0.29
27X-3, 10–12	245.20	33.60	1.62	–0.41
27X-3, 30–32	245.40	33.61	1.73	–0.08
27X-3, 40–42	245.50	33.61	1.66	–0.17
27X-3, 60–62	245.70	33.61	1.77	0.15
27X-3, 80–82	245.90	33.62	1.86	–0.52
27X-3, 100–102	246.10	33.62	1.84	0.02

Note: * = age based upon linear sedimentation rates constrained by the occurrence of the lower Chron 13n transition at 241.8 ± 1 mbsf and the upper transition at 213.5 ± 0.2 mbsf.